OPTICAL POTENTIAL APPROACH FOR LOW-ENERGY ELECTRON ELASTIC FORWARD AND BACKWARD SCATTERING BY Be, Mg, Ca, AND Yb ATOMS

E. Yu. REMETA, V. I. KELEMEN, Yu. Yu. BILAK[1], L. L. SHIMON[1]

Institute of Electron Physics, Nat. Acad. Sci. of Ukraine *(21, Universitetska Str., Uzhgorod 88000, Ukraine),* [1]Uzhgorod National University *(46, Pidhirna Str., Uzhgorod 88000, Ukraine)*

UDC 539.186.2

‰ 2002

Elastic low-energy (below 2 eV) electron scattering by alkaline-earth atoms and rare-earth itterbium atom to the energy-dependent intervals of angles of the forward and backward hemispheres is briefly considered. Energy dependences $S(E)$ that characterize scattering to the above intervals and are experimentally measured by using a hypocycloidal electron spectrometer are calculated. Using the ^2P- (Be, Mg) and ^2D- (Ca, Yb) shape resonances, as an example, their different influence on the function $S(E)$ is demonstrated. Graphical comparison of the theoretical values of $S(E)$ and the total elastic and differential cross sections is carried out.

1. The mechanism of shape- and Feshbach-resonance formation in electron scattering by atoms (ions) at low (about a few eV) energies is responsible for a strong interaction between incident and atomic electrons. The most important component of the general optical potential (OP) of this interaction, which can be calculated in various approaches, is due to the polarization potential responsible for deformation properties (monopole, dipole, and quadrupole) of the electron shell of a target atom [1 – 12].

Precise investigation of the low-energy structure in electron-atom scattering cross sections, and, hence, the potentials of their interaction requires a modification of experimental methods. This modification is necessary to perform precise studies of the scattering process in more detail. A technique using a hypocycloidal electron spectrometer (HES) was applied in [13] to study the peculiarities of low-energy (< 2 eV) electron scattering by Ca atoms. The scattering occurs at the collision energy E dependent interval of angles, and the energy dependence $S(E)$ is measured. Earlier, a trochoidal spectrometer was also used to measure the total cross sections. The function $S(E)$ is neither total elastic nor elastic differential scattering cross sections, but occupies a certain intermediate place.

Such a nature of $S(E)$ provides an essential advantage as compared to the above cross sections measured, in some cases, with considerable difficulties, because it allows the preliminary observation of the features in electron-atom (ion) scattering. The shortcoming of $S(E)$ is that the angular interval of measuring $S(E)$ is defined by the experimental parameters. This shortcoming, however, provides a certain advantage to experimental studies since it allows this interval to be varied by a simple selection of some parameters. Note that the less the angular interval, the better the function $S(E)$ reflects the differential peculiarities of the scattering.

Taking into account the mentioned above, it is evident that a thorough theoretical (preferably analytical) analysis of the energy dependences under study and their components can be done considering them as the functions of collision energy and scattering characteristics. Such an analysis is being carried out permanently within last years (see [14 – 16 and references therein]). Its goal is to show the possibility of using the measured energy dependence $S(E)$ in studying the peculiarities of the low-energy interaction with atoms during the scattering process. The possibility to determine the value and behaviour of the differential cross section is also important. In addition, this analysis may serve as a basis for understanding the physics of the electron interaction with ions and surfaces in the experiments with the use of HES (see references in [14]).

In this work, electron scattering by several atoms of group II and rare-earth Yb atoms is briefly reviewed in the OP approach. OP [4, 5, 13, 17] takes into account that Ca and Yb atoms, unlike Be and Mg, have a stable negative ion in the ns^2np configuration. Thus, ^2P- and ^2D-resonances are revealed in the low-energy electron scattering by Be, Mg [17] and Ca, Sr, Ba, Yb, respectively [4, 5]. Hence, it is quite important to compare the origin of the P- and D-resonances in the energy dependence $S(E)$.

2. The function $S(E)$ is related to the differential scattering cross section [4, 5, 13]

$$S(E) = 2\pi \int_{\theta_1}^{\theta_2} d\theta \sin\theta \frac{d\sigma(E, \theta)}{d\theta}. \qquad (1)$$

The boundary angles θ_1 and θ_2 are the functions of electron energy E. In the case of the elastic electron scattering with the experimental technique that uses

HES, the scattering angle is defined by the following relation to the experimental parameters [13, 14, 18, 19], in the particular case of the point-like electron beam entrance to the collision region:

$$\theta(E) = \arcsin\sqrt{\frac{eU_A - K/D^2}{E}}, \quad K = \frac{E_r}{B}L\left(\frac{2e}{m}\right)^{-1/2}. \tag{2}$$

In this formula, D is a spatial electron shift in the analyzer drift region, E_r and B are the electric and magnetic field strengths, respectively, L is an analyzer length, U_A is an analyzer potential, and e, m are electron charge and mass, respectively. If the analyzer has the $\Delta D = D_2 - D_1$ wide exit aperture, then an electron will pass the analyzer provided it was scattered within the $\Delta\theta = \theta_1(D_2) - \theta_2(D_1)$ angular range.

Thus, the energy dependences of angles for the scattering in the forward and backward hemispheres are, respectively:

$$\theta_{1,2}(E) = \arcsin(a_{1,2}/E)^{1/2},$$

$$\theta_{1,2}(E) = 180^\circ \mp \arcsin(b/E)^{1/2}. \tag{3}$$

The values $a_{1,2}, b$ are related to the experimental conditions considered above and to the characteristics from (2). To study the electron backscattering from metal ions and thin films, all the HES components are used similarly to the case of scattering from atoms (see references in [14]). However, the position of the analyzer with respect to the collision chamber is changed [18].

In [13, 19], the elastic electron scattering by Ca atoms was investigated in the energy-dependent mode. In this case, the analyzer potential was $U_A = 0.55$ V, and the respective constants were $a_1 = 0.482$ eV, $a_2 = 0.508$ eV. For the measurements at small energies, this potential is decreased and, for $U_A = 0.20$ V, $a_1 = 0.0949$ eV, $a_2 = 0.155$ eV. The angular curves $\theta_{1,2}(E)$ from (3) are presented in [16] (see also [14, 15]) with above two angular intervals of electron scattering to the forward hemisphere. At the initial energies, the values of angles for the above-mentioned constants $a_{1,2}$ are as follows: $E = 0.508$ eV — $\theta_1 \approx 77^\circ$, $\theta_2 = 90^\circ$; $E = 0.155$ — $\theta_1 \approx 51.6^\circ$, $\theta_2 = 90^\circ$. At the final energy $E = 2$ eV — $\theta_1 \approx 29.4^\circ$, $\theta_2 = 30.3^\circ$; $\theta_1 \approx 12.6^\circ$, $\theta_2 = 16.2^\circ$ for both constants, respectively. As we see, the value of 90°, at which the Legendre polynomial $P_1(\cos\theta) = 0$, is at the upper boundary of each interval only for the initial energy value. The magic angle 54.7°, for which $P_2(\cos\theta) = 0$, lies inside these intervals both at the initial energy and with increase in the energy. At $E > 0.76$ eV (for the first angular interval) and $E > 0.235$ eV (for the second one), this angle goes beyond the boundaries. On scattering in the backward hemisphere for $b = 0.1$ eV (see the respective curves in figures in [15, 16]) and at the initial energy $E = b - \theta_1 = 90^\circ$, $\theta_2 = 270^\circ$ and at the final $E = 2$ eV — $\theta_1 \approx 167^\circ$, $\theta_2 \approx 193^\circ$.

From the partial wave expansion for the scattering amplitude and from (1), one can easily obtain the following general expression for $S(E)$ [14, 16]:

$$S(E) = \sum_l \sigma_l(E)\, Q_{ll}(E) + \frac{\pi}{E}\sum_{l,l'>l}\sqrt{(2l+1)(2l'+1)}\times$$

$$\times\,[\eta_l \sin 2\bar{\delta}_l \cdot \eta_{l'} \sin 2\bar{\delta}_{l'} +$$

$$+\,(1 - \eta_l \cos 2\bar{\delta}_l)(1 - \eta_{l'} \cos 2\bar{\delta}_{l'})]\, Q_{ll'}(E). \tag{4}$$

Here, $\bar{\delta}_l(E)$ is the real part and $\eta_l(E)$ is connected with the imaginary part of the phase shift $\delta_l(E) = \bar{\delta}_l(E) + i\bar{\eta}_l(E)$, $\eta_l = \exp(-2\bar{\eta}_l)$; $\sigma_l(E)$ is the elastic partial cross section; energy-dependent functions $Q_{ll'}(E)$ are related to the Legendre polynomials $P_l(\cos\theta)$ [14 — 16]. Functions $Q_{ll'}(E)$ have a very important meaning, because they play the role of Legendre polynomials in the energy-dependent $S(E)$ and describe the scattering kinematics in this formalism. Note that, for standard scaterring angles ($\theta_1 = \theta$, $\theta_2 = \pi$), $S(E)$ coincides with the elastic cross section.

If, in some partial wave l, the resonance may occur, then it is convenient, similarly to the case of differential and total cross sections [20], to present the energy dependence (4) in the following potential-resonance form:

$$S(E) = S^{\text{pot}}(E) + S_l^r(E). \tag{5}$$

In (5), $S^{\text{pot}}(E)$ describes only the potential part of electron scattering (for real OP),

$$S^{\text{pot}}(E) = \frac{1}{2\pi}\sum_{s,t}\sqrt{(2s+1)(2t+1)}\times$$

$$\times \sin\delta_s \sin\delta_t \cos(\delta_s - \delta_t)\, Q_{st}(E), \tag{6}$$

and the second term describes the resonance side of scattering (a resonance with energy E_l^r and width Γ_l), which defines the structure of the energy dependence $S(E)$:

$$S_l^r(E) = \frac{\Gamma_l}{2}\frac{A_l(E)(E - E_l^r) + B_l(E)\,\Gamma_l/2}{(E - E_l^r)^2 + \Gamma_l^2/4}. \tag{7}$$

The antisymmetric $A_l(E)$ and symmetric $B_l(E)$ amplitudes in (7) have the following forms:

$$A_l(E) = -\frac{\sqrt{2l+1}}{4\pi}[\sqrt{2l+1}\sin 2\delta_l^0 Q_{ll}(E) + 2\sum_{s\neq l}\sqrt{2s+1}\sin\delta_s\cos(2\delta_l^0-\delta_s)Q_{sl}(E)],$$

$$B_l(E) = \frac{\sqrt{2l+1}}{4\pi}[\sqrt{2l+1}\cos 2\delta_l^0 Q_{ll}(E) - 2\sum_{s\neq l}\sqrt{2s+1}\sin\delta_s\sin(2\delta_l^0-\delta_s)Q_{sl}(E)]. \quad (8)$$

In (8), δ_l^0 is the potential (or background) part of the resonance phase shift [14, 16] (sign '0" indicates the potential part of this phase, i.e. the important value that defines the interference of the potential and resonance scattering types). In [20], partition (5) and expression (7) were suggested to analyze the total and differential experimental cross sections for the resonance electron scattering by atoms aimed at the possible determination of the resonance characteristics and value of δ_l^0 and at the investigation of the potential and resonance scattering interference.

Note that, as calculations of the phase function [4, 5] showed, the value of δ_l^0 for $l \geq 2$ at low energies is quite small (< 0.01 rad) for alkaline-earth atoms indicating a weak penetration of d- and higher partial waves inside the target atom and, therefore, the weak attractive and strong repulsive potential action of the effective (together with the centrifugical term) OP on these waves.

We can see from (7) that the resonance existing in the l-th wave can lead to the nonmonotonous behaviour of $S_l^r(E)$ (and $S(E)$) revealed as a minimum and maximum. In this case, the energy position of the resonance lies between these extrema. The non-monotonuos character is defined by amplitudes (8), whose energy dependence is, to a certain extent, due to the functions $Q_{ll'}(E)$. This will take place even if $\delta_l^0 = 0$ or $\pi/2$, whereas the total cross section has only a minimum or maximum [20], respectively, in this case.

The phase shifts $\delta_l(E)$ [4, 5, 17] used in the present paper were calculated with the help of the complex or real OP within the framework of the variable phase function method. OP of electron interaction with the target atom has the following form (see [1 – 5, 21 and references therein]) (in atomic units $h = e = m_e = 1$):

$$V_{\text{opt}}(r, E) = V_R(r, E) + iV_{\text{abs}}(r, E), \quad (9)$$

where the real part is

$$V_R(r, E) = V_S(r) + V_X(r, E) + V_{\text{pol}}(r). \quad (10)$$

$V_S(r)$ is the static potential of the atom, which describes the direct electrostatic interaction of the incident electron with the nucleus (with charge Z) and electron shells (with electron density $\rho(r)$):

$$V_S(r) = -\frac{Z}{r} + V_H(r), \quad V_H(r) = \int d\mathbf{r}'\frac{\rho(\mathbf{r}')}{|\mathbf{r}-\mathbf{r}'|}. \quad (11)$$

The exchange potential $V_X(r, E)$ in (10) is calculated in the local approximation for the exchange interaction between the incident electron and target electrons. It is also defined in the free-electron gas approximation with the local Fermi momentum for atomic electrons $k_{\text{F}}(r)$ as

$$V_X(r, E) = -\frac{k_{\text{F}}(r)}{\pi}\left(1 + \frac{1-\xi^2}{2\xi}\ln\left|\frac{1+\xi}{1-\xi}\right|\right),$$

$$k_{\text{F}}(r) = [3\pi^2\rho(r)]^{1/3}, \quad (12)$$

and

$$\xi = k_S(r)/k_{\text{F}}(r), \quad k_S(r) = k^2 + k_{\text{F}}^2(r) + 2I/[1 + (kr)^2/2], \quad k^2 = 2E. \quad (13)$$

Here, I stands for the ionization potential.

The polarization potential $V_{\text{pol}}(r)$ describes the effects of deformation of the target electron shell under influence of the incident electron. When modelling the dipole and quadrupole deformation, this potential is

$$V_{\text{pol}}(r, r_c) = -\alpha_d(0)W_6(r, r_c)/2r^4 - \alpha_q(0)W_8(r, r_c)/2r^6, \quad (14)$$

where $\alpha_d(0), \alpha_q(0)$ are the dipole and quadrupole static polarizabilities, and r_c is an adjustable parameter. The restricted function $W_m(r, x)$ is defined as

$$W_m(r, x) = 1 - \exp[-(r/x)^m]. \quad (15)$$

The absorption potential $V_{\text{abs}}(r, E)$ differs from zero only for the energies higher than the inelastic threshold. This potential takes into account the absorption effects in the approximation of quasifree electron scattering with the Pauli blocking:

$$V_{\text{abs}}(r, E) = -\upsilon_{\text{loc}}(r, E)\rho(r)\sigma_b(r, E)/2, \quad (16)$$

where the local speed of the scattered electron is

$$\upsilon_{\text{loc}}(r, E) = \{2[E - V_S(r) - V_X(r, E)]\}^{1/2}. \qquad (17)$$

The total cross section σ_b for Pauli-allowed electron-electron collision events is

$$\sigma_b(r, E) = [4\pi/5Ek_{\text{F}}^3(r)]\, f(r, E),$$

$$f = \begin{cases} f_1, \Delta + k_{\text{F}}^2(r) \le E, \\ f_1 + f_2, \Delta + k_{\text{F}}^2(r)/2 \le E \le \Delta + k_{\text{F}}^2(r), \\ 0, E \le \Delta + k_{\text{F}}^2(r)/2, \end{cases} \qquad (18)$$

where

$$f_1 = 5k_{\text{F}}^3(r)/2\Delta - k_{\text{F}}^3(r) \times$$

$$\times [10E - 3k_{\text{F}}^2(r)]/[2E - k_{\text{F}}^2(r)]^2,$$

$$f_2 = 2^{7/2}[k_{\text{F}}^2(r) + \Delta - E]^{5/2}/[2E - k_{\text{F}}^2(r)]^2$$

and Δ is the energy gap between the ground and first excited states of the target. Its values for Be, Mg, Ca and Yb are 2.73, 2.71, 1.88 , and 2.14 eV, respectively.

The electron density $\rho(r)$ and, consequently, the static potential $V_S(r)$ are determined in the ordinary approximations widely used in the atomic-structure calculations: the Thomas – Fermi approximation with various corrections and fitting parameters, Hartree – Fock (Hartree) method, the density functional theory (as in our case), and others. These approximations can also include some relativistic corrections. Note, that no partitioning of the atomic (ionic) target electrons into the valence electrons and core electrons is performed, in this OP approach, and the incident electron interacts with the whole shell.

Frequently, the analytic expressions or equations for the potentials V_X, V_{pol}, and V_{abs} can contain the fitting parameters, which are determined from the available spectroscopic characteristics of the system under consideration. In our calculations of phase shifts for Ca and Yb [4, 5], only one adjustable parameter r_c is used and is found from the condition that the negative Ca^- or Yb^- ion (and, similarily, Sr^- and Ba^-) exists with the affinity energy of 43 ± 7 and 54 ± 27 meV, respectively (see ref. in [4, 5]).

Phase shifts for Be and Mg atoms in [1] (used in this paper) were calculated by means of the dipole polarization potential similar to that in (14) but without the restriction function W_6. In [1, 2], this potential was used for the same distance r_0, the value of which was found from the condition of equality of the polarization and centrifuginal potentials. At small distances ($< r_0$), the potential is proportional to r. Note here that in [3] the total scattering cross section at low (< 5 eV) electron energies and differential one at intermediate (10, 20, 40 eV) electron energies were calculated for a Mg atom with the use of the adiabatic polarization potential.

3. The first numerical evaluation of $S(E)$ and its comparison with the experiment ($a_1 = 0.482$ eV, $a_2 = 0.508$ eV) (see the respective curve in the Figure for Ca atom) were carried out in [4, 5, 13] for the electron scattering by Ca to the forward hemisphere. Its nonmonotonous behaviour in the resonance region ($E_2^r = 0.87$ eV, $\Gamma_2 = 0.98$ eV) was revealed and the maximum $S(E)$ value at $E = 1.2$ eV coincides with the experimental one.

The analytical description of $S(E)$ [14] was applied for the forward electron scattering by Ca, and the analysis clearly demonstrates that its shape is related to the kinematic (angular) and dynamic (resonance) peculiarities of the scattering process. The shape of $S(E)$ in this work was analyzed due to the description via the direct, interference, resonance, and nonresonance terms. The term-to-term inclusion of partial waves in the calculation of $S(E)$ has revealed a minimum and maximum of this function, starting from the d-wave inclusion. $S(E)$ has only qualitatively some features specific of the elastic $\sigma(E)$ and differential $d\sigma/d\theta$ cross sections.

In [16], the theoretical function $S(E)$ for the forward ($a_1 = 0.482$ eV, $a_2 = 0.508$ eV for Sr and Ba and $a_1 = 0.0949$ eV, $a_2 = 0.155$ eV for Ba only) and backward ($b = 0.1$ eV for both atoms) electron scattering by Sr, Ba is considered. Important influence of the ^2D-resonances ($E_2^r = 0.60$ eV, $\Gamma_2 = 0.68$ eV; $E_2^r = 0.34$ eV, $\Gamma_2 = 0.13$ eV, respectively) on $S(E)$ was demonstrated. Moreover, in the Ba atom case due to the small resonance energy, a qualitatively coinsidence for $S(E)$, $\sigma(E)$ and $d\sigma/d\theta$ was demonstrated using the small values of $a_{1,2}$ for a possible experiment. Electron scattering by these atoms to the backward hemisphere of angles is also defined by the ^2D-resonance, especially in the Ba atom case.

In [17], the ^2P-resonances for Be and Mg atoms were calculated in the OP approach, and then more accurate calculations gave the following parameters: $E_1^r = 0.40$ eV, $\Gamma_1 = 0.84$ eV and $E_1^r = 0.25$ eV, $\Gamma_1 = 0.84$ eV, respectively, defined from the energy phase shifts behaviour. In [1], for these atoms (Be, Mg) in the so-called static-exchange-polarization approximation, the following values of parameters were obtained only for the ^2P-resonances: $E_1^r = 0.195$ eV, $\Gamma_1 = 0.283$ eV and $E_1^r = 0.161$ eV, $\Gamma_1 = 0.283$ eV, respectively. In [2], these values were obtained more

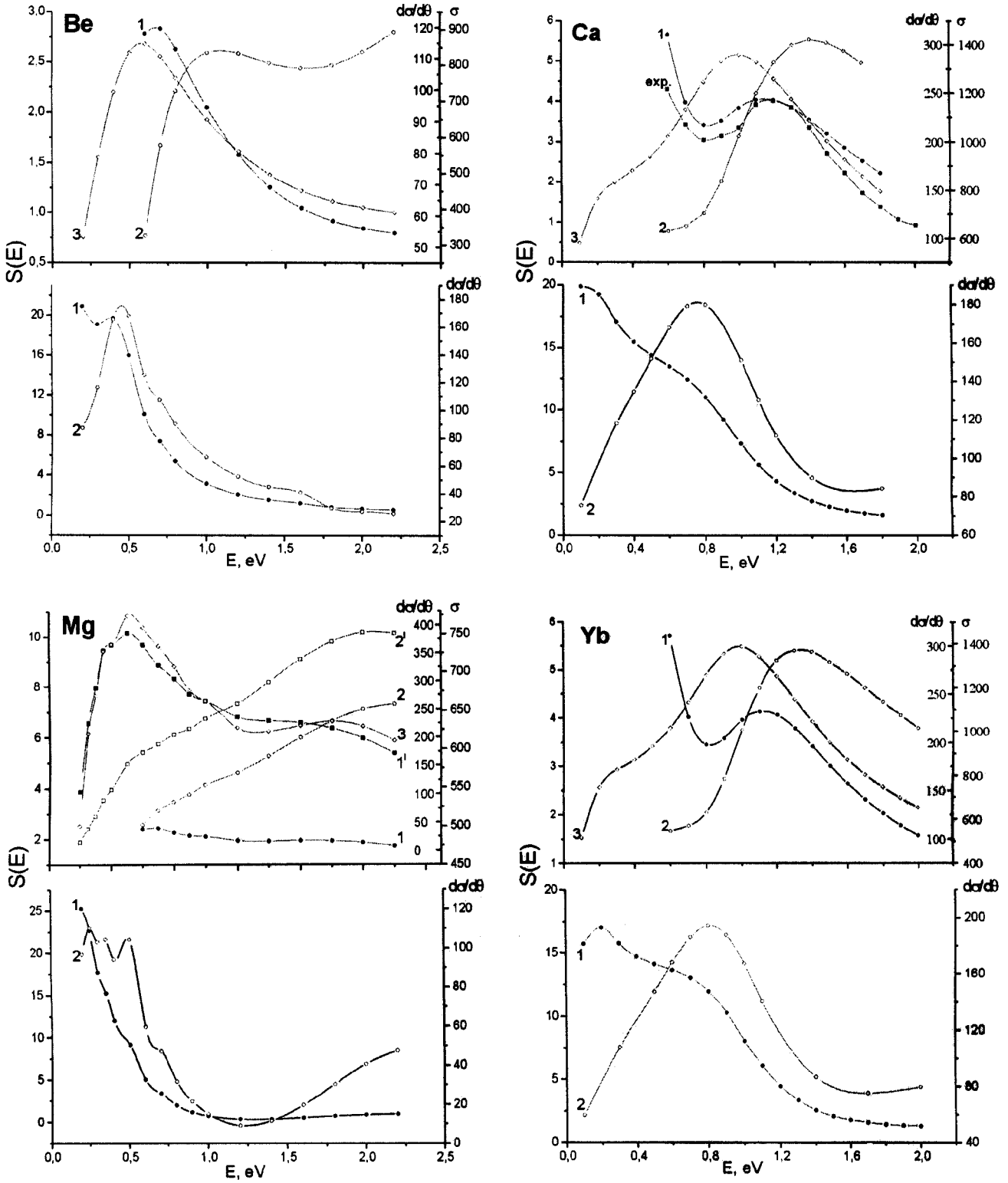

Energy dependences $S(E)$ (*1*), differential $d\sigma/d\theta$ (*2*) (for the average angle value and at 180°), and total elastic $\sigma(E)$ (*3*) cross sections (in atomic units) for electron scattering by Be, Mg, Ca, Yb atoms to the forward (upper part) and backward (bottom) hemispheres of angles. *1, 2* $a_1 = 0.482$ eV, $a_2 = 0.508$ eV; *1′, 2′* $a_1 = 0.0949$ eV, $a_2 = 0.155$ eV

accurately due to the expansion in the function basis and to the use of more accurate polarizability values. The following values of parameters of the ^2P- (for Be, Mg) and ^2D- (for Mg) resonances were obtained: Be $E_1^r = 0.14$ eV, $\Gamma_1 = 0.13$ eV; Mg $E_1^r = 0.14$ eV, $\Gamma_1 = 0.24$ eV; $E_2^r = 1.74$ eV, $\Gamma_2 = 3.27$ eV. Also the following resonance parameters of the ^2P- and ^2D-resonances were obtained for the Ca atom: $E_1^r = 0.06$ eV, $\Gamma_1 = 0.10$ eV; $E_2^r = 0.70$ eV, $\Gamma_2 = 0.57$ eV.

In [22], the ^2P-resonance for Be at 0.13 eV was calculated by the close-coupling method. But, for Mg atom, the ^2P-resonance was not obtained because of the small number of channels used. In [21, 23], the R-matrix method with pseudostates was applied to obtain the ^2P-resonance in Mg at the 0.17 energy giving a good coincidence with the experimental data at 0.16 eV [24] and 0.15 eV [25].

As seen, the theoretical results are defined to a great extent by the approximation used. The first-principle calculations are quite labour-consuming.

Note that, in the theoretical works [11, 12], the function $S(E)$ for the electron scattering by Ca atoms calculated and measured in [4, 5, 13] has been erroneously identified with the total elastic cross section. In [11, 12], our $S(E)$ was normalized to the calculated cross section and not considered as a new independent and additional experimental characteristic, inherent in the novel methods using HES. Calculations in [11] were carried out in the close-coupling approximation for six S, P, D singlet and triplet states with the use of the R-matrix method. In [12], for e-Ca scattering, the influence of core-valence electron correlations was studied. The calculations were carried out in the close-coupling approximation for five states of a Ca atom (three singlet (S, P, D) and two triplet (P, D) ones) and with the use of the R-matrix method. In [11], the ^2D-resonance was calculated at $E_2^r = 1.2$ eV, while, in [12], it was calculated without the above-mentioned correlations at $E_2^r = 1.1$ eV and with correlations at 1.3 eV.

In Figure, we present the dependences $S(E)$, $d\sigma/d\theta$, and $\sigma(E)$ for the electron scattering to the forward (upper part) and backward (bottom) hemispheres by Be, Mg for three partial waves and by Ca, Yb for five partial waves. The energy dependence of differential cross sections was calculated for the average angle $\theta(E) = [\theta_1(E) + \theta_2(E)]/2$.

Forward scattering. Electron scattering by Be, Mg atoms is characterized by the ^2P-shape resonance with the above-mentioned parameters [17]. The shape of $S(E)$ for the scattering by Be and Mg is similar to $\sigma(E)$. For the initial (0.6 – 0.7 eV) energy values (for $a_1 = 0.482$ eV, $a_2 = 0.508$ eV), it is defined by Q_{00}, Q_{01} [15] with maxima in this region. The contribution from Q_{11} is small. The coincidence of $S(E)$ and $\sigma(E)$ in the Mg case is better for $a_1 = 0.0949$ eV, $a_2 = 0.155$ eV ((see Mg in Figure and compare curves *1*, *1′* for $S(E)$ and *2*, *2′* for $d\sigma/d\theta$), and the contribution from Q_{11} is larger. This agrees with the similar behaviour of $S(E)$ for Ba [16]. Zero value of the Legendre polynomial $P_1(\cos\theta)$ at 90° (initial energy value) plays no role, probably, due to the fact that this angle lies at the end of the interval. One more possible reason is the large width of the angular interval at the initial energy, i.e., ~ 13° and 38° for different $a_{1,2}$.

The functions $S(E)$ for the electron scattering by Ca and Yb ($a_1 = 0.482$ eV, $a_2 = 0.508$ eV) are similar because the resonances in these cases have the same parameters (Ca $E_2^r = 0.87$ eV, $\Gamma_2 = 0.98$ eV; Yb $E_2^r = 0.89$ eV, $\Gamma_2 = 0.89$ eV). The shape of $S(E)$ for the scattering by Ca and Yb is very different from $\sigma(E)$ because of the zero values of Q_{2i} ($i = 0 \div 4$) at 0.7 eV [15] (from the magic angle 54.7°) that defines the nonmonotonous character of $S(E)$ and indicates the ^2D-resonance. A difference between $S(E)$ and $d\sigma/d\theta$ remains very large. The angular interval width is small in this case, ~ 2.5 – 3°.

Backward scattering. At the initial (0.1 – 0.3 eV) energy values, the functions $Q_{ij}(E)$ ($i, j = 0, 1$) [15] play a principal role in the shape of $S(E)$ for Be, Mg. However, the behaviour of Q_{00} (> 0) almost coincides with Q_{01} (< 0), and the main contribution is due to Q_{11}.

Q_{2i} functions (see [14, 15]) have more complicated behaviour: zero values, extreme points (positive and negative) reflected in $S(E)$ for Ca and Yb. The shape of $S(E)$ partially coincides with $d\sigma/d\theta$ at 180°.

Most likely, just the large width of the angular interval within the entire energy range, including resonance energies, does not allow one to reveal them effectively by means of the functions $S(E)$.

4. The resonance mechanism of the electron scattering by atomic systems is very clearly defined from the energy dependences $S(E)$. The low-energy resonances on the scattering to the forward hemisphere should be found by means of $S(E)$ with the smallest values of the constants $a_{1,2}$.

Peculiarities of $S(E)$ for the forward scattering show an evidence for the resonance interaction properties better than those in the total elastic or differential cross sections. The manifestation of the ^2P- and ^2D-resonances in this function is very different, and this favours their identification in scattering processes.

Nevertheless, one has to calculate the phase shifts and $S(E)$ functions with optical potentials, in which the polarization and exchange potentials are calculated in different approximations. This will stimulate new experiments on electron-atom scattering, including those angular intervals (e.g., converging to some chosen angles: 54.7, 90, 120°) that will allow one to find clearly both the resonance and other peculiarities of the interaction process.

The nonmonotonous energy behaviour of $S(E)$ resulted from (7) may be revealed only in the form of a maximum due to the influence of the kinematic term $Q_{ll'}(E)$.

The energy dependence $S(E)$ for backward scattering has no nonmonotonous features due to the resonances and is characterized by a monotonous decrease with increase in the collision energy.

We are grateful to Dr. A.V.Snegursky for very helpful discussion.

1. *Kurtz H.A., Öhrn Y.*//Phys. Rev. 1979. **A19.** P.43 48.
2. *Kurtz H.A., Jordan K.D.*//J. Phys. B.: Atom and Mol. Phys. 1981. **14.** P.4361 4376.
3. ¥†¥‡¥· . ., ¡⁄ . ., µ¢£ ·¤¸ . .// . 1989. **34,** ”3. .345 349.
4. ¥†¥‡¥· . ., ¥‡¥É . ., ¡⁄ . .// ¤§¤– Ô¥–É µ·Ò ¤ É‡·Ò ,É‡–·µ¢¥·¤°: ¡. ,ÉÉ°. .- ¥É•¡°•£: §⁄. ¤‡. . µ¸¥, 1991. ”12. .152 161.
5. *Kelemen V.I., Remeta E.Yu., Sabad E.P.*//J. Phys. B.: Atom and Mol. Opt. Phys. 1995. **28.** P.1527 1546.
6. •¤¡ –¤· . ., ¢ ·µ¢ . ., ˚¸¤¥¢ . .// ¤§¤– Ô¥–É µ·Ò ¤ É‡·Ò ,É‡–·µ¢¥·¤°: ¡. ,ÉÉ°. .- ¥É•¡°•£: §⁄. ¤‡. . µ¸¥, 1991. ”12. .77 88.
7. ‡˚,Ö . ., µ·¤¢–¥• . ., ¥•¥¶–µ¢ . . ¤ ⁄•.// . 1985. **55.** .2304 2309.
8. ¥›Ö† . ., ¢•µ–¤° . ., ¡⁄ . .// ¥µ¤Ö •¥§µ·,-·Ò Ö†¥·¤° ¢ Ô¥–Éµ·µ É‡·Ò ,É‡–·µ¢¥·¤Ò ¤¥¢: ˚–. ⁄˚‡–, 1988.
9. *Yuan J., Zhang Z., Wan Hong*//Phys. Rev. A. 1990. **41.** P.4732 4739.
10. *Yuan J., Zhang Z.*//Ibid. 1990. **42**. P.5363 5373.
11. *Yuan J., Fritsche L.*//Ibid. 1997. **55,** N2. P.1020 1027.
12. *Yuan J., Lin C.D.*//Ibid. 1998. **58**, N4. P.2824 2827.
13. µ‡·Õ .Ù ¶¥·¤– . . É Ø// . 1992. **37**, ”11. .1639 1647.
14. ¥‡¥É . ., ¶¥·¤– . ., ¤†– . .// . 2001. **71**, ¢¶.4. .13 22.
15. ¤†– . .// Ø. ƒ£µ. ⁄¥•ƒ. ˚·-É. 1999. ”5. .180 185.
16. ¥‡¥É . ., ¤†– . ., ¤‡µ . .// . 2001. **46**, ”5. .627 633.
17. *Kelemen V.I., Remeta E.Yu., Sabad E.P.*//Proc. 16th ICPEAC, New York, July 26 August 1 1989. P.868.
18. ¶¥·¤– . . ¤ ⁄•.// . 1998. ”1. .109 117.
19. µ‡·Õ . ., ¶¶ . ., ¥•·Ù¢ . . ¤ ⁄•.// ¤§¤– Ô¥–É· µ· · Ò¡ ¤ É‡· · Ò¡ ,É‡†–· µ¢¥· ¤°: ¡. ,É É¥°. .- ¥-É¥•¡°•£: §⁄. ¤‡. . µ¸¥, 1991. ”12. .174 186.
20. ¥⁄¢¥¥¢ . ., •¤¢,–¤° . . ¡ ¤·É¥•¸¥•¥·˝¤¤ •¥§µ·,-·µ£µ ¤ ¶µÉ·˝¤ †Ù£µ • ,,¥Ö¤°. I ⁄·µ· · †ÙÒ •¥§µ·,. ¤¥¢, 1982. (•¥¶•. -82).
21. *Lengyel V., Zatsarinny O., Remeta E.*// Electron Scattering on Complex Atoms (Ions). New York: Nova Science, 2000. (Horizons in World Physics. Vol 234).
22. ¡•¤– ·É . .// É‡· Ò¥¶• µ˝ ¥, ,Ò: ¡ , É É¥° . ¤£ : ¤-· É¥, 1975. .80 123.
23. *Gedeon V., Lengyel V. et al.*// Phys. Rev. A. 1999. **59**. P.2016 2030.
24. *Burrow P.D., Comer J.J.*//Physica. 1975. **B8**. L92.
25. *Romanyuk N.I., Shpenik O.B., Zapesochny I.P.*//Pis'ma Zh. Tekh. Fiz. 1980. **6**. P.877 880.

Received 13.10.00,
revised version 12.11.01